Olefin Copolymerization via Controlled Radical Polymerization: Copolymerization of Acrylate and 1-Octene

Rajan Venkatesh,[†] Simon Harrisson,[‡,§] David M. Haddleton,[‡] and Bert Klumperman*,[†]

Dutch Polymer Institute, Department of Polymer Chemistry, Eindhoven University of Technology, Den Dolech 2, P.O. Box 513, 5600 MB Eindhoven, The Netherlands, and Department of Chemistry, University of Warwick, Coventry, CV4 7AL, UK

Received December 23, 2003; Revised Manuscript Received March 23, 2004

ABSTRACT: The atom transfer radical copolymerization (ATRP) of methyl acrylate (MA) with 1-octene was investigated in detail. Well-controlled copolymers containing almost 25 mol % of 1-octene were obtained using ethyl 2-bromoisobutyrate (EBriB) as initiator. Narrow molar mass distributions (MMD) were obtained for the ATRP experiments. The feasibility of the ATRP copolymerizations was independent of the ligand employed. Copolymerizations carried out using 4,4′-dinonyl-2,2′-bipyridine (dNbpy) resulted in good control, with significant octene incorporation in the polymer. The lower overall percent conversion obtained for the dNbpy systems as compared to that of the PMDETA systems was attributed to the redox potential of the formed copper(I)−ligand complex. The comparable free radical (co)polymerizations (FRP) resulted in broad MMD. An increase in the fraction of the olefin in the monomer feed led to an increase in the level of incorporation of the olefin in the copolymer, at the expense of the overall percent conversion. There was a good agreement between the values of the reactivity ratios determined for the ATRP and FRP systems. The formation of the copolymer was established using matrix-assisted laser desorption/ionization−time-of-flight−mass spectrometry (MALDI−TOF−MS). From the obtained MALDI−TOF−MS spectra for the ATRP systems, several units of 1-octene were incorporated in the polymer chain, and only one pair of end groups was observed. On comparison, in the FRP systems, due to the multitude of side reactions occurring, several end groups were obtained. In general, narrow chemical composition distributions were obtained for the ATRP systems as compared to FRP.

Introduction

Copolymers of α-olefins with polar monomers remain a pivotal area in polymer research, since the effect of incorporation of functional groups into an otherwise nonpolar material is substantial.[1,2]

In the area of metal-catalyzed insertion polymerization, the Brookhart Pd-based diimine catalyst[3] copolymerizes ethylene and higher α-olefins with acrylates and vinyl ketones.[4] Other late-transition-metal-based complexes are also known to tolerate the presence of polar functional groups.[5] Block copolymers of ethylene with acrylates and methacrylates using group 4 metals are known.[6] Recently published reviews cover the work in this field.[7] However, statistical copolymerization of these two types of monomers is difficult to achieve due to the very unfavorable reactivity ratios in conjunction with these catalyst systems. Recent developments from Novak[8] indicated that olefins could be copolymerized with vinyl monomers via a free radical mechanism. This was followed up by a communication indicating the feasibility of the copolymerization of methyl acrylate (MA) with 1-alkenes using copper-mediated controlled polymerization.[9]

ATRP[10,11] is one of the techniques employed to obtain living (or controlled) radical polymerization. In copper-mediated ATRP, the carbon−halogen bond of an alkyl halide (RX) is reversibly cleaved by a $Cu^{I}X$/ligand system, resulting in a radical (R*) and $Cu^{II}X_2$/ligand (deactivator). The radical will mainly either reversibly deactivate, add monomer, or irreversibly terminate (Scheme 1, eqs 1−8).

This paper is a very detailed study on the copolymerization of an α-olefin (1-octene) with an acrylate (methyl acrylate, MA). Comparison of reaction kinetics between free radical polymerization (FRP) and atom transfer radical polymerization (ATRP) was carried out. A heterogeneous transition metal/ligand system was employed for the ATR polymerizations. Reactivity ratios were measured using an online NMR technique. ^{1}H nuclear magnetic resonance (NMR) spectroscopy was employed to monitor the individual monomer conversion over time, similar to work reported by Haddleton et al.[12] The reaction was carried out within the cavity of the NMR spectrometer. From the data obtained, the reactivity ratios were calculated. The effect of monomer feed composition and of ligand was investigated. Chemical composition distributions (CCDs) were assessed using mass spectrometry for both ATRP and conventional free radical polymerization (FRP).

Experimental Section

Materials Methyl acrylate (MA, Merck, 99+%) and 1-octene (Oct, Aldrich, 98%) were distilled and stored over molecular sieves. *p*-Xylene (Aldrich, 99+% HPLC grade) was stored over molecular sieves and used without further purification. *N*,*N*,*N*′,*N*′′,*N*′′-Pentamethyldiethylenetriamine (PMDETA, Aldrich, 99%), 4,4′-dinonyl-2,2′-bipyridine (dNbpy, Aldrich, 97%), ethyl 2-bromoisobutyrate (EBriB, Aldrich, 98%), copper(I) bromide (CuBr, Aldrich, 98%), copper(II) bromide ($CuBr_2$, Aldrich, 99%), aluminum oxide (activated, basic, for column chromatography, 50−200 μm), tetrahydrofuran (THF, Aldrich, AR), and 1,4-dioxane (Aldrich, AR) were used as supplied. α,α′-Azobis(isobutyronitrile) (AIBN, Merch, >98%) was recrystallized twice from methanol before use. For online

---

[†] Eindhoven University of Technology.

[‡] University of Warwick.

[§] Current address: Department of Chemistry, Washington University, One Brookings Drive, CB 1134, St. Louis, MO, 63130.

10.1021/ma035986m CCC: $27.50

Scheme 1. General Scheme for ATRP[a]

Initiation

$$\mathrm{R{-}X} + \mathrm{Cu^{I}X/L} \underset{k_d^0}{\overset{k_a^0}{\rightleftharpoons}} \mathrm{R^*} + \mathrm{Cu^{II}X_2/L} \tag{1}$$

$$\mathrm{R^*} + \mathrm{M} \xrightarrow{k_p^0} \mathrm{P_1^*} \tag{2}$$

Propagation

$$\mathrm{P_n{-}X} + \mathrm{Cu^{I}X/L} \underset{k_d}{\overset{k_a}{\rightleftharpoons}} \mathrm{P_n^*} + \mathrm{Cu^{II}X_2/L} \tag{3}$$

$$\mathrm{P_n^*} + \mathrm{M} \xrightarrow{k_p} \mathrm{P_{n+1}^*} \tag{4}$$

Solubilization

$$\mathrm{Cu^{I}X/L_{sol}} \underset{k^{I}_{sol}}{\overset{k^{I}_{insol}}{\rightleftharpoons}} \mathrm{Cu^{I}X/L_{insol}} \tag{5}$$

$$\mathrm{Cu^{II}X_2/L_{sol}} \underset{k^{II}_{sol}}{\overset{k^{II}_{insol}}{\rightleftharpoons}} \mathrm{Cu^{II}X_2/L_{insol}} \tag{6}$$

Termination

$$\mathrm{P_m^*} + \mathrm{P_n^*} \xrightarrow{k_{tD}^{m,n}} \mathrm{D_m^H} + \mathrm{D_n^=} \tag{7}$$

$$\mathrm{P_m^*} + \mathrm{P_n^*} \xrightarrow{k_{tC}^{m,n}} \mathrm{D_{m+n}} \tag{8}$$

[a] R* and P_n* are radicals from initiator and polymer, respectively, R−X and P_n−X are halogen-terminated initiator and polymer chains with halide end group, M is monomer, D^H and $D^=$ are the dead polymer chain with a hydrogen and vinyl end group, respectively, and D_{m+n} are the dead chains formed as a result of termination via combination. Rate coefficients for activation (k_a), deactivation (k_d), propagation (k_p), solubilization (k_{sol}), insolubilization (k_{insol}), chain length dependent termination via combination ($k_{tC}{}^{m,n}$), and chain length dependent termination via disproportionation ($k_{tD}{}^{m,n}$).

NMR experiments, toluene-d_8 (Cambridge Isotope Labs Inc.) and toluene (Hi-Dry, anhydrous solvent, Romil Ltd.) were used as supplied. Copper(I) bromide (CuBr, Aldrich, 98%) was purified according to the method of Keller and Wycoff.[13]

Synthetic Procedures. a. ATR Copolymerization of MA and 1-Octene. A typical polymerization was carried out in a 100 mL three-neck round-bottom flask. *p*-Xylene (23.2 g), MA (4.67 g, 5.42 × 10^{-2} mol), 1-octene (6.1 g, 5.4 × 10^{-2} mol), CuBr (0.19 g, 1.3 × 10^{-3} mol), and $CuBr_2$ (0.07 g, 3 × 10^{-4} mol) were accurately weighed and transferred to the flask. The ligand PMDETA (0.29 g, 1.7 × 10^{-3} mol) was then added. The reaction mixture was degassed by sparging with argon for 30 min. The flask was immersed in a thermostated oil bath kept at 80 °C and stirred for 10 min. A light green, slightly heterogeneous system was obtained. The initiator, EBriB (0.65 g, 3.3 × 10^{-3} mol), was added slowly via a degassed syringe. The reactions were carried out under an argon atmosphere. Samples were withdrawn at suitable time periods throughout the polymerization. A predetermined amount of the sample was transferred immediately after withdrawal into a GC vial and diluted with 1,4-dioxane, so as to determine the monomer conversion using GC. The remaining sample was diluted with THF and passed through a column of aluminum oxide prior to SEC and MALDI−TOF−MS measurements.

b. Free Radical Copolymerization of MA and 1-Octene. A typical polymerization was carried out in a 25 mL three-neck round-bottom flask. *p*-Xylene (11.6 g), MA (2.33 g, 2.7 × 10^{-2} mol), and 1-octene (3.04 g, 2.7 × 10^{-2} mol) were accurately weighed and transferred to the flask. The reaction mixture was degassed by sparging with argon for 30 min. The flask was immersed in a thermostated oil bath kept at 80 °C. The initiator AIBN (0.02 g, 1.7 × 10^{-4} mol) was dissolved in a minimum amount of *p*-xylene, and the initiator solution was added slowly via a degassed syringe. The reactions were carried out under a flowing argon atmosphere. Samples were withdrawn at suitable time periods throughout the polymerization. A predetermined amount of the sample was transferred immediately after withdrawal into a GC vial and diluted with 1,4-dioxane, so as to determine the monomer conversion using GC. The remaining sample was diluted with THF, prior to SEC and MALDI−TOF−MS measurements.

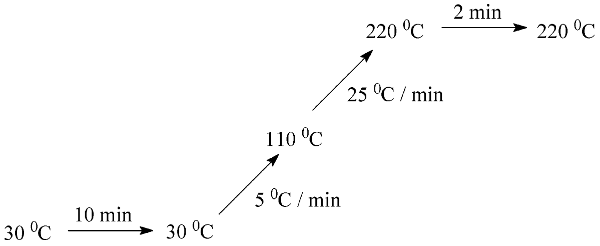

Figure 1. GC temperature gradient.

c. Online NMR Experiments. In a typical ATRP, CuBr (0.03 g, 2 × 10^{-3} mol) and $CuBr_2$ (0.01 g, 4 × 10^{-5} mol) were added to a predried Schlenk tube, which was sealed with a rubber septum. The tube was evacuated and flushed with nitrogen three times to remove oxygen. Then MA (1.4 g, 1.6 × 10^{-2} mol), 1-octene (0.6 g, 5 × 10^{-3} mol), toluene-d_8 (4.0 g), toluene (0.2 g), PMDETA (0.05 g, 3 × 10^{-4} mol), and EBriB (0.13 g, 6.7 × 10^{-4} mol) were added via oven-dried, degassed syringes. The liquid reagents in the Schlenk tube were degassed by three freeze−pump−thaw cycles. An aliquot of 2 mL of this solution was transferred to a NMR tube. So as to detemine the initial monomer concentration at the onset of the reaction, the first scan at time = 0 s was taken at room temperature, before heating the sample to the required reaction temperature. After the experiment, the sample was diluted with THF and passed through a column of aluminum oxide prior to SEC.

Analysis and Measurements. a. Laboratory Experiments. *Determination of Conversion and MMD.* Monomer conversion was determined from the concentration of residual monomer measured via gas chromatography (GC). A Hewlett-Packard (HP-5890) GC equipped with an AT-Wax capillary column (30 m × 0.53 mm × 10 μm) was used. *p*-Xylene was employed as the internal reference. From repetitive runs, the estimated relative error in the determination of monomer conversion value is 5%. The GC temperature gradient used is given in Figure 1.

Molar mass (MM) and molar mass distributions (MMD) were measured by size exclusion chromatography (SEC) at ambient temperature using a Waters GPC equipped with a Waters model 510 pump, a model 410 differential refractometer (40 °C), a Waters WISP 712 autoinjector (50 μL injection volume), a PL gel (5 μm particles), a 50 × 7.5 mm guard column, and a set of two linear columns (Mixed-C, Polymer Laboratories, 300 × 7.5 mm, 5 μm bead size, 40 °C). THF was used as the eluent at a flow rate of 1.0 mL/min. Calibration was carried out using narrow MMD polystyrene (PS) standards ranging from 600 to 7 × 10^6 g/mol. The MM was calculated using the universal calibration principle and Mark−Houwink parameters[14] [PMA: $K = 1.95 \times 10^{-4}$ dL/g, $a = 0.660$; PS: $K = 1.14 \times 10^{-4}$ dL/g, $a = 0.716$]. The molecular weights were calculated relative to PMA homopolymer. The estimated error in the molecular weight averages when using this approach is 10%. Data acquisition and processing were performed using Waters Millenium 32 software.

NMR. ^{1}H and ^{13}C nuclear magnetic resonance (NMR) spectra were recorded on a Varian 400 spectrometer in deuterated chloroform ($CDCl_3$) at 25 °C. All chemical shifts are reported in ppm downfield from tetramethylsilane (TMS), used as an internal standard ($\delta = 0$ ppm). NMR was done to determine the copolymer composition (^{1}H NMR) and to confirm whether octene is incorporated into the copolymer chains (^{13}C NMR).

MALDI−TOF−MS. Measurements were performed on a Voyager-DE STR (Applied Biosystems, Framingham, MA) instrument equipped with a 337 nm nitrogen laser. Positive-ion spectra were acquired in reflector mode. Dithranol was chosen as the matrix. Sodium trifluoroacetate (Aldrich, 98%) was added as the cationic ionization agent. The matrix was dissolved in THF at a concentration of 40 mg/mL. Sodium trifluoroacetate was added to THF at typical concentrations of 1 mg/mL. The dissolved polymer concentration in THF was approximately 1 mg/mL. For each spectrum 1000 laser shots were accumulated. In a typical MALDI experiment, the matrix, salt, and polymer solutions were premixed in the ratio: 5 μL sample:5 μL matrix:0.5 μL salt. Approximately 0.5 μL of the obtained mixture was hand-spotted on the target plate.

b. Online NMR Experiments. *NMR*. ^{1}H NMR spectra were recorded on a Bruker ACP 400 spectrometer. Polymerization kinetics followed by ^{1}H NMR were recorded using the Bruker built-in kinetics software. Toluene (Hi-Dry) was employed as the internal reference.

Determination of MMD. Molar mass (MM) and molar mass distributions (MMD) were measured by size exclusion chromatography (SEC) at ambient temperature using a Polymer Laboratories system. For SEC-1 [high MM], THF/triethylamine (95:5) was used as the eluent at a flow rate of 1.0 mL/min, with a Polymer Laboratories (PL-gel) 5 μm (50 × 7.5 mm) guard column. A set of two linear columns [Mixed-C, Polymer Laboratories, 5 μm (300 × 7.5 mm)] with a refractive index detector was employed. Calibration was carried out using narrow polydispersity poly(methyl methacrylate) (PMMA) standards ranging from 200 to 1.577×10^6 g/mol. For SEC-2 [low MM], THF was used as the eluent at a flow rate of 1.0 mL/min, with a Polymer Laboratories (PL-gel) 3 μm (50 × 7.5 mm) guard column. A set of two linear columns [Mixed-E, Polymer Laboratories, 3 μm (300 × 7.5 mm)] with a refractive index detector was employed. Calibration was carried out using narrow polydispersity PMMA standards ranging from 200 to 2.8×10^4 g/mol. MM was calculated by comparing the samples with the PMMA standards and by using Mark–Houwink parameters[15] [PMA: $K = 1.95 \times 10^{-4}$ dL/g, $a = 0.660$; PMMA: $K = 9.55 \times 10^{-5}$ dL/g, $a = 0.719$].

Results and Discussion: Copolymerization

The synthesis of the copolymers and comparison of the ATRP results with the conventional free radical systems will be examined. The influence of the monomer feed composition and of the ligand will be highlighted. Determination and comparison of the obtained reactivity ratios from ATRP and FRP are carried out using online NMR technique. Detailed chemical composition distributions (CCDs) for the copolymers synthesized by ATRP, determined by MALDI–TOF-MS, are discussed. The various end groups obtained during the free radical reactions are assigned, and their mode of production is explained. An interesting pattern in the sequence distribution of the monomers, obtained from the MALDI data, is examined.

Copolymerization of MA/1-Octene Copolymers. AIBN-initiated and ATR copolymerization of MA and 1-octene were examined as summarized in Table 1.

Table 1. Copolymers of MA/1-Octene

entry[a]	mole fraction of octene in monomer feed (f_{Oct})	mole fraction of octene incorporated (F_{Oct})[e]	molar mass (M_n) (g/mol)[f]	polydispersity index (M_w/M_n)[f]
1*[b]	0.25	0.12	2.5×10^3	1.3
2#[c]	0.25	0.12	8.2×10^3	3.5
3*[b]	0.50	0.26	2.0×10^3	1.3
4#[c]	0.50	0.24	6.2×10^3	2.8
5*[d]	0.25	0.09	1.8×10^3	1.2

[a] * = ATRP reactions; # = free radical polymerization (FRP) using AIBN as initiator. [b] Targeted $M_n = 3000$ g/mol; [monomer]:[EBriB]:[CuBr]:[PMDETA] = 32:1:0.5:0.5; reaction time = 22 h; reaction temperature = 80 °C. [c] AIBN (10 mmol/L); reaction time = 22 h; reaction temperature = 80 °C. [d] Targeted $M_n = 3000$ g/mol; [monomer]:[EBriB]:[CuBr]:[dNbpy] = 32:1:0.5:1; reaction time = 48 h; reaction temperature = 80 °C. [e] Calculated from values obtained from GC measurements and proton NMR. [f] Determined by size exclusion chromatography relative to polystyrene standards using refractive index detector. Volume ratio solvent:monomer = 2:1.

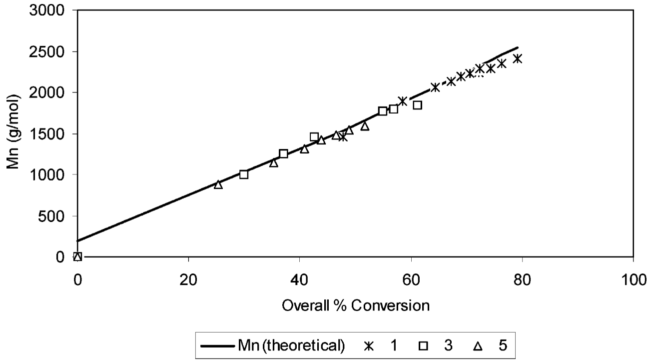

Figure 2. Plot of M_n vs overall conversion for the ATRP copolymerizations of MA–octene. Labels: **(1)** $f_{\mathrm{Oct}} = 0.25$, **(3)** $f_{\mathrm{Oct}} = 0.50$. Targeted $M_n = 3000$ g/mol; [monomer]:[EBriB]:[CuBr]:[PMDETA] = 32:1:0.5:0.5; **(5)** $f_{\mathrm{Oct}} = 0.25$. Targeted $M_n = 3000$ g/mol; [monomer]:[EBriB]:[CuBr]:[dNbpy] = 32:1:0.5:1.

Some observations can be made from the data in Table 1:

(i) 1-Octene copolymerizes via a free radical mechanism. Homopolymerization of 1-octene was attempted in both FRP and ATRP, but no polymer was obtained. This could be attributed to the fact that α-olefins undergo degradative chain transfer of allylic hydrogens.[15] The stable allylic radical derived from the monomer is slow to reinitiate and prone to terminate.

(ii) Copolymerizations under FRP conditions produce relatively low molecular weight polymer compared to MA homopolymerization under similar conditions.[16] The tendency for 1-octene to behave as a chain transfer agent under FRP conditions has been reported for MMA systems.[17]

(iii) The experimentally determined MMs for polymerizations under ATRP conditions are close to the calculated values (Figure 2). The linearity clearly indicated that there were a constant number of growing chains during the polymerization.

(iv) Narrow MMDs were obtained in the ATRP experiments, which suggests conventional ATRP behavior, with no peculiarities caused by the incorporation of 1-octene.

(v) As the fraction of the α-olefin was increased in the monomer feed, its incorporation was higher in the copolymer (compare entries 1 and 3, 2 and 4). Two effects can cause this phenomenon. Because of composition drift, the fraction of 1-octene in the remaining monomer increases, which leads to a decrease in average propagation rate constant. When the fraction 1-octene increases, the probability of end-capping an octene moiety at the chain end with a bromide increases. When this happens, the chain will be virtually inactive, since there are no substituent groups in octene to stabilize the formed radical. Hence, the ATRP equilibrium prefers to be on the dormant side. Thus, increasing the mol % of α-olefin in the monomer feed decreased the overall conversion (compare entries 1 and 3, 2 and 4 in Table 1 and Figure 3).

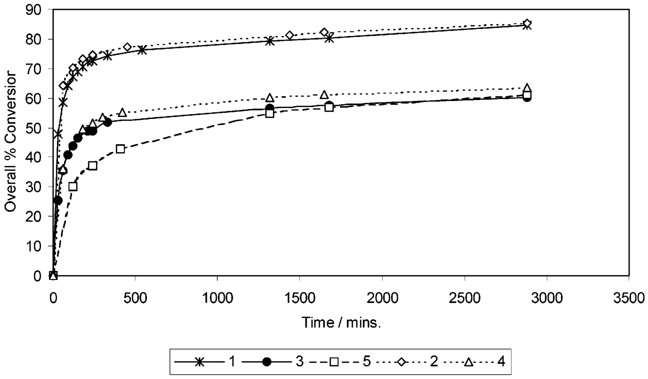

Figure 3. Plot of overall conversion vs time for MA−octene copolymerizations. Labels: ATRP **(**1**)** $f_{\mathrm{Oct}} = 0.25$, **(**3**)** $f_{\mathrm{Oct}} = 0.50$. Targeted M_n = 3000 g/mol; [monomer]:[EBriB]:[CuBr]:[PMDETA] = 32:1:0.5:0.5; **(**5**)** $f_{\mathrm{Oct}} = 0.25$. Targeted M_n = 3000 g/mol; [monomer]:[EBriB]:[CuBr]:[dNbpy] = 32:1:0.5:1. FRP: **(**2**)** $f_{\mathrm{Oct}} = 0.25$, **(**4**)** $f_{\mathrm{Oct}} = 0.50$, AIBN (10 mmol/L).

Table 2. Copolymers of MA/1-Octene

entry[a]	mole fraction of octene in monomer feed (f_{Oct})	molar mass (M_n) (g/mol)[f]	polydispersity index (M_w/M_n)[f]
1*[b]	0.10	2.2 × 10³	1.1
2#[c]	0.10	32.4 × 10³	4.9
3*[b]	0.25	2.3 × 10³	1.1
4#[d]	0.25	11.0 × 10³	5.2
5*[b]	0.50	1.6 × 10³	1.2
6#[e]	0.50	14.3 × 10³	3.6

[a] * = ATRP reactions; # = free radical polymerization (FRP) using AIBN as initiator. Reaction temperature = 80 °C; solvent: monomer = 2:1 by volume. [b] Targeted M_n = 3000 g/mol; [monomer]:[EBiB]:[CuBr]:[PMDETA] = 32:1:0.5:0.5; reaction time = 12 h. [c] AIBN (3 mmol/L); reaction time = 9 h. [d] AIBN (10 mmol/L); reaction time = 9 h. [e] AIBN (3 mmol/L); reaction time = 12 h. [f] Determined by size exclusion chromatography relative to poly(methyl methacrylate) standards using refractive index detector.

(vi) It is largely coincidental that the rates of polymerization in ATRP and in conventional FRP shown in Figure 2 are nearly identical. The choice of initiator concentration and polymerization conditions happens to be such that this coincidence occurs. However, the fact that the ratios at which the two comonomers are consumed seem to be in close agreement points to a great similarity between the reactivity ratios. This will be further discussed below.

(vii) To indicate the feasibility of the copolymerization under homogeneous ATRP conditions, the copolymerization was also carried out using dNbpy as the ligand (Table 1, entry 5). This resulted in a good control over the polymerization. MM increased linearly with overall conversion (Figure 2), though the overall conversion and hence the incorporation of 1-octene were slightly lower as compared to those of the PMDETA systems. The lower the redox potential, the larger the apparent equilibrium constant for the oxidation of copper(I) to copper(II) and therefore the higher the activity in catalyzing the polymerization. The redox potential for a copper(I)−PMDETA complex was lower than that of the copper(I)−dNbpy complex; hence, the PMDETA systems exhibit a higher polymerization rate.[18]

Reactivity Ratios. AIBN-initiated and ATR copolymerization of MA with 1-octene, followed in situ by ^{1}H NMR, were examined as summarized in Table 2. The trend obtained for the copolymerization from the online NMR experiments (Table 2) was comparable to that observed in the laboratory-scale experiments (Table 1). Narrow MMDs were obtained for the ATRP experiments, suggesting conventional ATRP behavior with no peculiarities caused by the incorporation of 1-octene.

Individual monomer conversions were monitored online using NMR. Figure 4 shows sample spectra of the polymerizing mixture after various reaction times (0−540 min). To quantify the results and track the fractions of the two monomers in the residual monomer mixture, the various vinylic protons were integrated with respect to the protons present in the aromatic region from toluene, which was employed as the internal standard. Integration of the signals yields relative amounts of residual monomer in the polymerization mixture. These amounts can easily be converted into comonomer fractions. The fraction of MA in the residual monomer was plotted as a function of overall monomer conversion (Figure 5). This type of experimental data can be described by the integrated copolymerization equation, also known as the Skeist equation (eq 9).[19]

$$\xi = 1 - \left(\frac{f_A}{f_A^0}\right)^{r_B/(1-r_B)}\left(\frac{1-f_A}{1-f_A^0}\right)^{r_A/(1-r_A)}\left(\frac{f_A^0-\delta}{f_A-\delta}\right)^{(1-r_B)/(2-r_A-r_B)} \tag{9}$$

where ξ is the fractional total conversion on a molar basis, f_A^0 is initial mole fraction of monomer A based on the total amount of monomer, and δ is the following function of the monomer reactivity ratios, r_A and r_B (eq 10):

$$\delta = \frac{1 - r_A r_B}{(1 - r_A)(1 - r_B)} \tag{10}$$

From Figure 5, **(**i**)** an increase in the fraction of 1-octene in the monomer feed leads to a decrease in the overall conversion. **(**ii**)** As the fraction of MA in the monomer feed was decreased, there is a better accordance for the monomer conversion between FRP and ATRP reactions (compare 5 and 6, 1 and 2). The deviation is much larger between 1 and 2 as compared to 5 and 6. Deviations from the steady-state ratio between the two propagating radicals may occur during the initial stages of an ATR copolymerization.[20] This is also most likely the origin of the observed deviations between ATRP and conventional free radical copolymerization in this case. Additional research is currently being carried out in our labs to prove the general character of this phenomenon in living radical copolymerization.

The data from Figure 5 can be used to estimate the reactivity ratios. The best way of estimating reactivity ratios from experimental data is via the use of a nonlinear least-squares method.[21] The method of choice in the present work calculates the sums of squares in a relevant r_1−r_2 space.[22,23] The minimum in the r_1−r_2 sum of squares surface is then easily found. This point estimate is used to calculate the drawn curves shown in Figure 5. The 95% joint confidence intervals are subsequently determined as the curve of intersection between the r_1−r_2 sum of squares surface and a horizontal plane, the height of which is determined according to a method previously described.[22] The estimated relative error in copolymer composition from NMR is 5%. The resulting point estimates and confidence intervals for the six different experiments are shown in

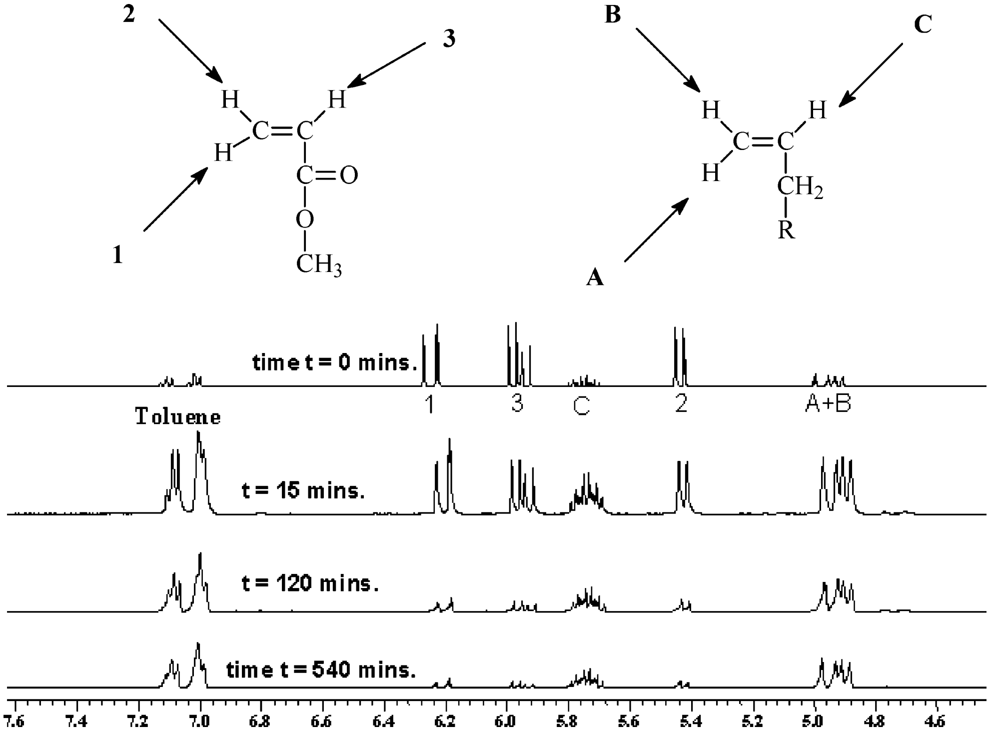

Figure 4. ^{1}H NMR spectra of a MA–1-octene copolymerization, measured on line during the polymerization experiment (free radical polymerization: $f_{\mathrm{Oct}} = 0.25$; AIBN = 10 mmol/L; reaction time = 9 h; reaction temperature = 80 °C).

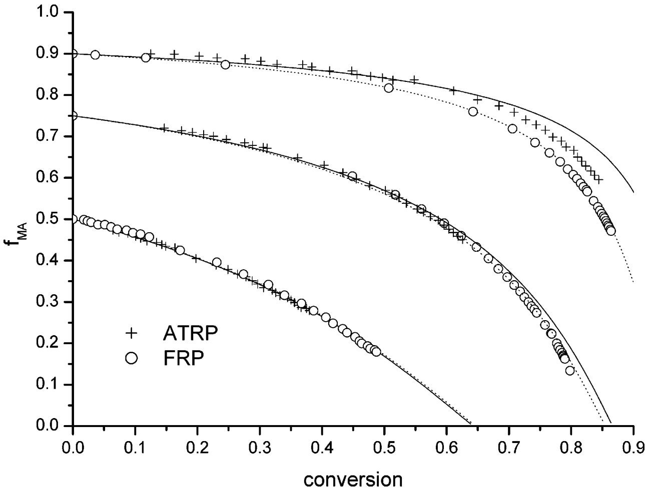

Figure 5. Plot of fraction of MA in the residual monomer as a function of overall monomer conversion. Solid lines are best fits according to the reactivity ratio point estimates as given in Table 3 for ATRP experiments. Dotted curves are the equivalent for conventional free radical copolymerizations.

Figure 6. The point estimates are summarized in Table 3. Experiment 1 (ATRP, $f_{\mathrm{Oct}} = 0.10$) is poorly described by the Skeist equation. The uncertainty in the reactivity ratios for this experiment is correspondingly larger than that of the other experiments. As indicated above, the most probable explanation for this observation is the more frequently observed deviation from steady-state equilibrium in ATR copolymerization. The fact that this deviation from steady-state equilibrium mainly takes place in the initial stages of the polymerization, and the poor agreement is mainly observed in the later stages is explained by the rather shallow decrease of the fraction MA in the early stages of the polymerization.

Polymer Characterization. The synthesized copolymers were characterized using matrix-assisted laser desorption/ionization–time-of-flight–mass spectrometry (MALDI–TOF–MS). In a previous publication, SEC and NMR were primarily used for the copolymer characterization.[8,9] Determination of the accurate (relative) molar masses of synthetic polymers is often difficult to achieve. Detailed information on molecular structure, such as identification of end groups, can be even more difficult. Even though polymers with a molecular weight of several hundred thousand daltons can be characterized by MALDI–TOF–MS, most of the investigations with this technique focus on the mass range where single polymer chains are resolved.[24] The resolved mass range depends on the molar mass range of the repeating units and on the resolution of the mass spectrometer. In favorable cases, the polymer composition can be deduced directly from the absolute mass of each signal of the polymer distribution.

MALDI–TOF–MS spectra allow the determination of the variation in chemical composition between individual copolymer chains and comparison of the chemical composition distribution (CCD) in different mass ranges, coupled with very clear peak assignment with respect to end group, theoretical mass, and isotopic mass distribution.

Atom Transfer Radical Polymerization. Figure 7 shows the MALDI–TOF–MS spectrum for the MA/1-octene copolymer (Table 1, entry 1). The overlap of several distributions is clearly visible. This is typical for the resolved mass distribution of a copolymer and is due to the heterogeneity of the degree of polymerization, corresponding to the chain length distribution, coupled with the heterogeneity in the chemical composition.

Figure 8 is an expansion of a selected portion of the spectrum shown in Figure 7. The peak assignments of Figure 8, described in Table 4, are made using the following strategies: (i) comparison with the homopolymer spectrum of MA, (ii) comparison of the experimental masses and those theoretically calculated, and (iii)

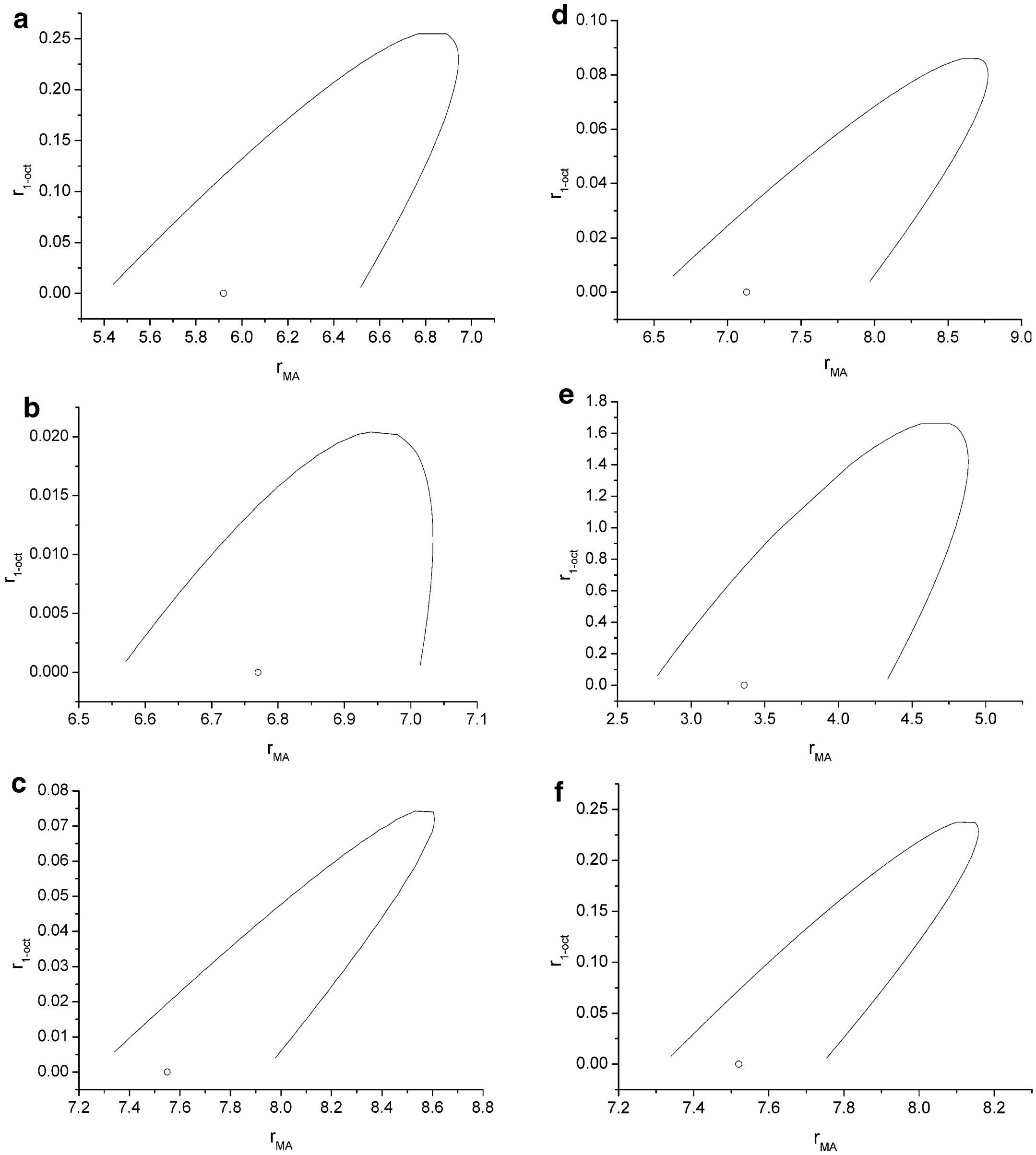

Figure 6. Point estimates and confidence intervals for the different copolymerizations calculated using the method described in the text. Reaction temperature = 80 °C. Solvent:monomer volume ratio = 2:1. (a) ATRP with a fraction 1-octene in the feed $f_{\mathrm{Oct}} = 0.25$. Further conditions: targeted $M_n = 3000$ g/mol; [monomer]:[EBiB]:[CuBr]:[PMDETA] = 32:1:0.5:0.5; reaction time = 12 h. (b) FRP with $f_{\mathrm{Oct}} = 0.25$; AIBN (10 mmol/L); reaction time = 9 h. (c) ATRP with $f_{\mathrm{Oct}} = 0.50$; for conditions see (a). (d) FRP with $f_{\mathrm{Oct}} = 0.50$; AIBN (3 mmol/L); reaction time = 12 h. (e) ATRP with $f_{\mathrm{Oct}} = 0.10$; for conditions see (a). (f) FRP with $f_{\mathrm{Oct}} = 0.10$; AIBN (3 mmol/L); reaction time = 9 h.

Table 3. Determined Reactivity Ratios for MA/1-Octene

entry[a]	mole fraction of MA in monomer feed (f_{MA})	mole fraction of octene in monomer feed (f_{Oct})	r_{MA}	$r_{1-\mathrm{octene}}$
1*[b]	0.90	0.10	3.36	0
2#[c]	0.90	0.10	7.52	0
3*[b]	0.75	0.25	5.92	0
4#[d]	0.75	0.25	6.77	0
5*[b]	0.50	0.50	7.55	0
6#[e]	0.50	0.50	7.13	0

[a] * = ATRP reactions; # = free radical polymerization (FRP) using AIBN as initiator. [b] Targeted $M_n = 3000$ g/mol; [monomer]:[ebib]:[CuBr]:[PMDETA] = 32:1:0.5:0.5; Reaction time = 12 h. [c] AIBN (3 mmol/L); Reaction time = 9 h. [d] AIBN (10 mmol/L); Reaction time = 9 h. [e] AIBN (3 mmol/L); Reaction time = 12 h. Reaction temperature = 80 °C. Solvent:monomer volume ratio = 2:1.

comparison of the theoretical isotopic distribution with the observed distributions. The polymer chains were cationized with sodium and therefore were detected at a m/z value of 23 Da above the theoretically calculated mass.

After subtracting the mass of the cationization reagent, the detected signals should agree with the expected masses of the copolymer chains, which can be calculated according to eq 11:

$$M_{\mathrm{copo}} = 115.15 + [(m \times 86.09) + (n \times 112.21)] + 79.90 \quad (11)$$

where 115.15 and 79.9 are the average masses of the end groups from the initiator fragment and bromine, respectively (since EBriB was used as the ATRP initiator), 86.09 and 112.21 are the average masses of the MA and 1-octene repeating units, respectively, and m and n are the numbers of the monomers in the chain.

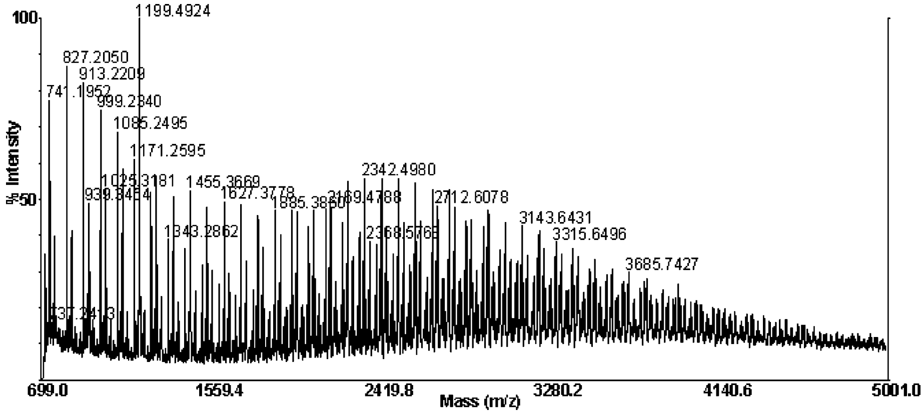

Figure 7. MALDI−TOF−MS spectrum for MA/Oct copolymer, $f_{\mathrm{Oct}} = 0.25$, $F_{\mathrm{Oct}} = 0.12$. Targeted M_n = 3000 g/mol; [monomer]:[EBriB]:[CuBr]:[PMDETA] = 32:1:0.5:0.5; reaction time = 22 h; reaction temperature = 80 °C (Table 1, entry 1) [spectrum acquired in the reflector mode; matrix: dithranol].

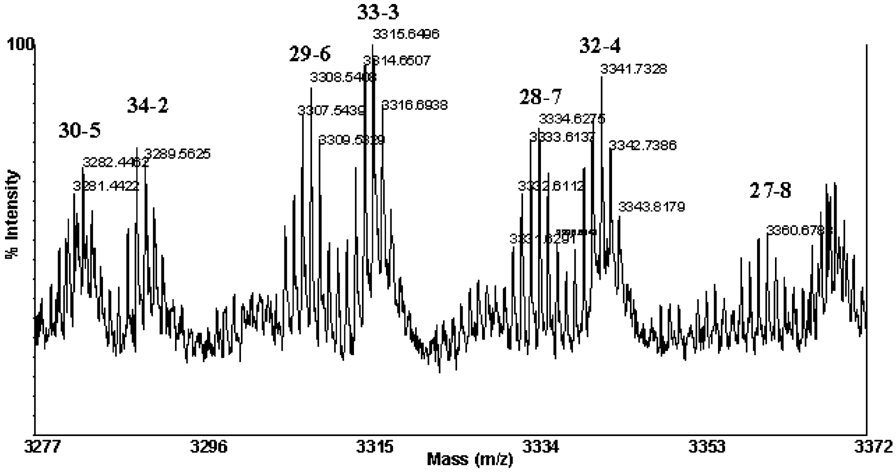

Figure 8. Expansion of the MALDI−TOF−MS spectrum for MA/Oct copolymer, $f_{\mathrm{Oct}} = 0.25$, $F_{\mathrm{Oct}} = 0.12$. Targeted M_n = 3000 g/mol; [monomer]:[EBriB]:[CuBr]:[PMDETA] = 32:1:0.5:0.5; reaction time = 22 h; reaction temperature = 80 °C (Table 1, entry 1) [spectrum acquired in reflector mode; matrix: dithranol].

Table 4. Peak Assignment of the MALDI−TOF−MS Spectrum Shown in Figure 8

peak no.	MA units	1-octene units	obsd mass (Da)	theor mass (Da)	Na^+
34-2	34	2	3289.56	3289.64	1
33-3	33	3	3315.65	3315.77	1
32-4	32	4	3341.73	3341.89	1
30-5	30	5	3282.44	3281.93	1
29-6	29	6	3308.54	3308.05	1
28-7	28	7	3334.62	3334.18	1
27-8	27	8	3360.67	3360.31	1

However, the agreement between the theoretical and observed masses is improved when eq 12 is employed. In this equation, the terminal bromine atom is not included.

$$M_{\mathrm{copo}} = 115.15 + [(m \times 86.09) + (n \times 112.21)] \quad (12)$$

During ATRP, most of the polymer chains are halide end-capped. This is of paramount importance since, in its absence, the reaction will be uncontrolled. It has been already shown in this paper that M_n increases linearly with overall conversion for the ATRP copolymerizations (Figure 3) and that a low PDI is obtained. Hence, the reaction is certainly well controlled, and this in turn indicates the presence of the halide at the copolymer chain end. In MALDI−TOF−MS, during ionization (in the range of laser intensity used in this work) it is observed that the terminal Br fragments. Other groups have already reported the loss of the HBr during MALDI−TOF−MS analysis of poly(acrylates) produced by ATRP.[25] A careful choice of the laser intensity is extremely important for the spectral quality in MALDI−TOF−MS. There is an obvious tradeoff between obtaining a spectrum with enough intensity (high laser power) and obtaining a spectrum without signs of fragmentation or distortions.[26]

The data in Table 4 demonstrate that several units of 1-octene were incorporated in the polymer chain. This indicates that the octene is behaving as a comonomer and not simply as a chain transfer agent, in which case at most two octene units would be observed. There is an excellent correlation between the theoretical mass and that experimentally observed, which further validates the presence of the olefin in the copolymer. Moreover, the theoretical isotopic mass distribution is in good agreement with the observed distribution (Figure 9). Since only one pair of end groups is evident, and no chains seem to have been initiated by octene radicals, it can be concluded that chain transfer to 1-octene in the targeted MM range is negligible.

It has been already established by ^{13}C NMR spectroscopy that in free radical copolymerziation the olefin was randomly distributed in the copolymer chain.[8,9] From

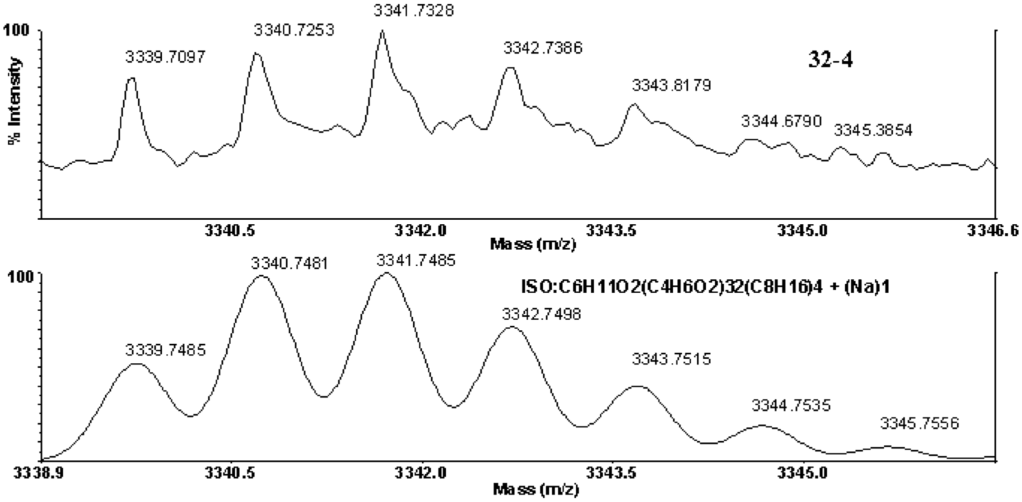

Figure 9. Details of the MALDI−TOF−MS spectrum of MA/Oct copolymer. $f_{\mathrm{Oct}} = 0.25$, $F_{\mathrm{Oct}} = 0.12$. Targeted M_n = 3000 g/mol; [monomer]:[EBriB]:[CuBr]:[PMDETA] = 32:1:0.5:0.5; reaction time = 22 h; reaction temperature = 80 °C (Table 1, entry 1). Isotopic mass distributions: observed (above) and theoretical below for a polymer chain.

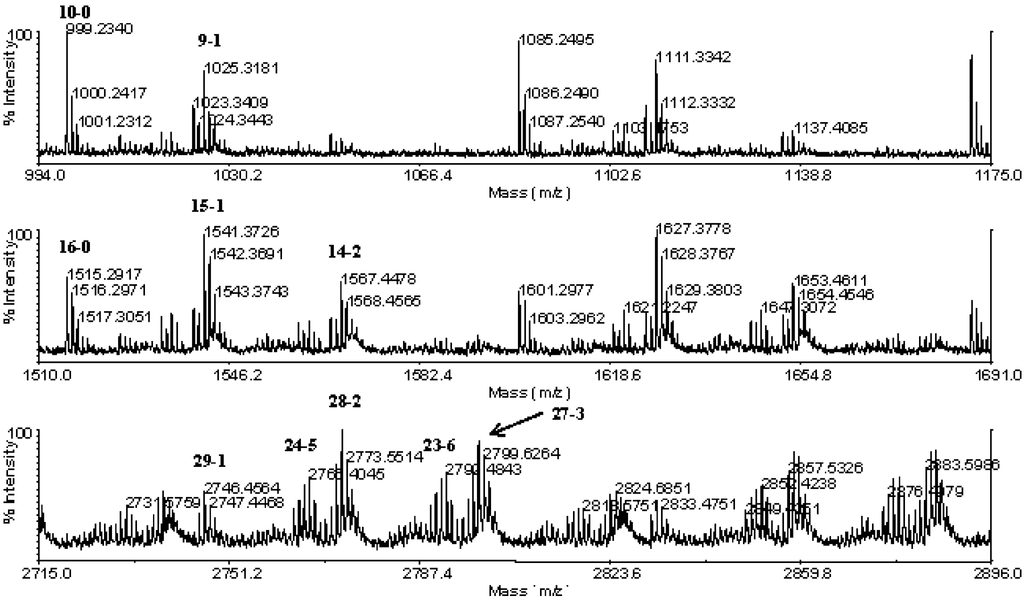

Figure 10. Expansion in different mass regions from a MALDI−TOF−MS spectrum of MA/Oct copolymer. $f_{\mathrm{Oct}} = 0.25$, $F_{\mathrm{Oct}} = 0.12$. Targeted M_n = 3000 g/mol; [monomer]:[EBriB]:[CuBr]:[PMDETA] = 32:1:0.5:0.5; reaction time = 22 h; reaction temperature = 80 °C (Table 1, entry 1) [spectrum acquired in reflector mode; matrix: dithranol].

the MALDI−TOF−MS data, a clear pattern in the sequence distribution is observed. This is achieved by selecting regions of increasing mass from the obtained MALDI−TOF−MS spectrum (Figure 7) and expanding them to similar scale ranges for easy comparison. The peak assignments are made using eq 12. From Figure 10, an interesting trend is observed. In the low MM region, the homopolymer peak of MA has the highest intensity. In the progressively higher MM regions, the copolymer peaks increase in intensity and the homopolymer peaks decrease in intensity. So, in essence, a gradient copolymer type pattern is observed. This was further confirmed by the copolymer fingerprint contour plots obtained for samples withdrawn at different time intervals during the ATR copolymerization (Supporting Information, Figure 1). There was a clear broadening observed in the contour plots for samples withdrawn at later stages during the copolymerization. From the plots, it was clear that as the copolymerization progressed, more octene was getting incorporated. Moreover, it is evident the number of octene units incorporated is greater than the expected number. That is, if for a polymer chain with a degree of polymerization (DP) of 10 say one unit of octene is incorporated, then for a chain with DP of 20, only 2 units should be expected to be incorporated. This most certainly is not the case.

The origin of a gradient-type comonomer incorporation has been discussed previously for the copolymerization of acrylate−methacrylate copolymerization. In that case, there is a large difference in the activation rate parameters between dormant chains that carry an acrylate terminal group versus those with a methacrylate terminal group. In the present case the situation is somewhat different, although the result is similar. It is likely that for propagating radicals with a terminal 1-octene unit the time constant for cross-propagation is smaller than that for deactivation. In other words, chains with a 1-octene terminal unit exclusively undergo cross-propagation. Relevant activation rate parameters for α-olefin copolymerizations will

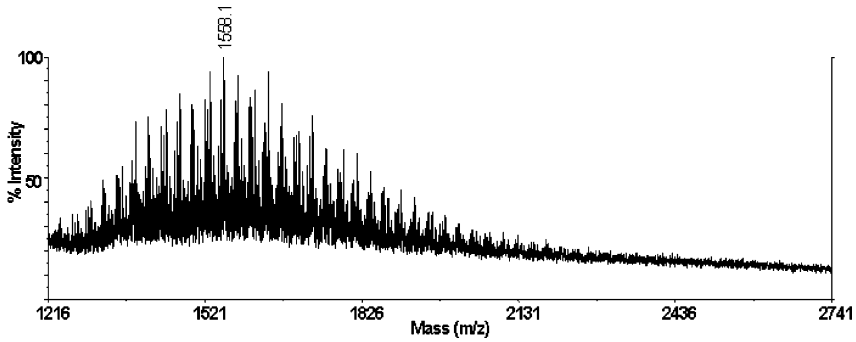

Figure 11. MALDI−TOF−MS spectrum of a fractionated SEC portion from the MA/Oct copolymer. AIBN (10 mmol/L); reaction time = 22 h; reaction temperature = 80 °C (Table 1, entry 2) [spectrum acquired in reflector mode; matrix: dithranol].

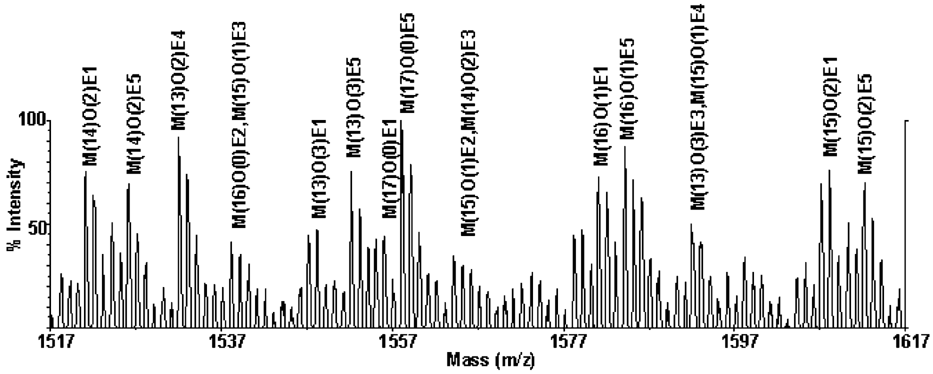

Figure 12. Expansion of the MALDI−TOF−MS spectrum acquired for the fractionated SEC portion from the MA/Oct copolymer (Table 1, entry 2) [spectrum acquired in reflector mode; matrix: dithranol].

be encompassed in a forthcoming paper. The resulting gradient in copolymer composition or the relationship between composition and molar mass may be interpreted as follows. At the onset of the copolymerization, predominantly homopolymerization of MA occurs (since MA is a more reactive monomer). During the copolymerization, due to composition drift, the fraction of 1-octene in the remaining monomer increases; hence, the probability of 1-octene being incorporated into the polymer chain increases. The addition of an α-olefin is followed by a very rapid cross-propagation, causing the chain that incorporates the α-olefin to gain chain length faster than the homo-MA chain.

Free Radical Polymerization. MM estimates provided by MALDI−TOF−MS agree with the values obtained by conventional techniques only in the case of samples with narrow MMD,[27] whereas with polydisperse polymers MALDI−TOF−MS does not give reliable results. Hence the polydisperse samples obtained in this work were fractionated by SEC, yielding narrow MMD samples which, when analyzed by MALDI−TOF−MS, gave good mass spectra.

Figure 11 depicts the MALDI−TOF−MS spectrum for a fractionated portion (by SEC) of a MA/Oct copolymer synthesized using AIBN as initiator (Table 1, entry 2). The copolymer was investigated to compare the CCD between the FRP and ATRP systems. Figure 12 is an expansion of a selected portion of the spectrum shown in Figure 11. The peak assignment in the FRP case is far more difficult than in the ATRP case. This is primarily due to the multitude of different end groups which are present, in addition to the heterogeneity normally present for copolymers.

The peak assignments were made using the following strategies: (i) predicting the possible end groups, which result normally during a free radical reaction; (ii) comparison of the observed mass with those theoretically calculated. The polymer chains were all cationized with sodium and hence were detected at a *m*/*z* value 23 Da above the theoretically calculated mass. All polymer chains were assigned to various chemical compositions, constituting of varying methyl acrylate (M) and octene (O) units. All the copolymer chains can be divided into having five pairs of end groups (E1, E2, E3, E4, E5). The different end groups observed originate from the various side reactions, which occur during conventional free radical polymerization.

End group 1 (E1) was obtained as a result of chain transfer to monomer or polymer. It has been shown that octene acts as a chain transfer agent during free radical polymerization [increasing the fraction of octene in the monomer feed, resulting in lower overall conversion and lower MM (Table 1, compare entries 2 and 4)]. Further, previous work in the area of chain transfer to polymer for acrylate monomers has clearly revealed that abstraction of the backbone proton from a dead polymer chain may take place.[28] The resulting end groups for the polymer chain can be assigned according to eq 13

$$M_{\text{copo}} = 68.09 + [(m \times 86.09) + (n \times 112.21)] + 1.00 \tag{13}$$

where 68.09 and 1.00 are the average masses of the end groups from the initiator fragment (2-cyanoprop-2-yl radical from AIBN) and the abstracted hydrogen from octene or dead polymer, respectively, 86.09 and 112.21 are the average masses of the MA and 1-octene repeating units, respectively, and *m* and *n* the numbers of the monomers in the chain.

The polymer chains having end group 2 (E2) were obtained due to termination via combination of the propagating chains. Solomon and Moad[29,30] conclude

Scheme 2. Mechanism for β-Scission[a]

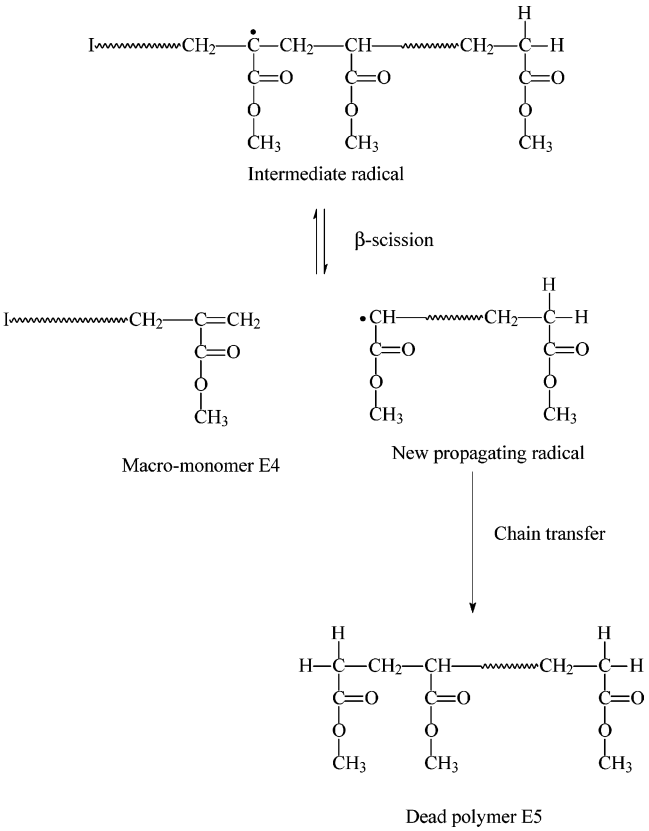

[a] I in end group E4 is the 2-cyanoprop-2-yl fragment from AIBN.

that despite the sparsity of reliable data, termination of polymerizations involving vinyl monomers occurs predominantly via combination. Equation 14 represents the product of termination via combination.

$$M_{\mathrm{copo}} = 68.09 + [(m \times 86.09) + (n \times 112.21)] + 68.09 \quad (14)$$

where 68.09 is the average mass of the end group from the initiator fragment (AIBN fragment), 86.09 and 112.21 are the average masses of the MA and 1-octene repeating units, respectively, and *m* and *n* the numbers of the monomers in the chain.

The octene radical formed via chain transfer to monomer can also initiate the polymerization, though the rate coefficient of initiation by this stable allylic radical is very slow. These initiated chains also terminate as a result of chain transfer from monomer or polymer (eq 15), producing end group 3 (E3).

$$M_{\mathrm{copo}} = 111.20 + [(m \times 86.09) + (n \times 112.21)] + 1.00 \quad (15)$$

where 111.20 and 1.00 are the average masses of the end groups from the octene allylic radical and the abstracted hydrogen from an octene or via chain transfer to polymer, respectively, 86.09 and 112.21 are the average masses of the MA and 1-octene repeating units, respectively, and *m* and *n* the numbers of the monomers in the chain.

Chain transfer to polymer occurring during free radical polymerization of acrylates can lead to β-scission in the temperature range 80−240 °C (Scheme 2).[31] Abstraction of a proton from a dead polymer chain backbone results in the formation of an intermediate radical, which in turn can undergo β-scission. As a result of this, a new propagating radical and a macromonomer are formed. The new propagating radical may also be terminated as a result of transfer events. Thus, two polymer chains with two different pairs of end groups are obtained. The polymer chains with end groups 4 (E4) and 5 (E5) were assigned as shown in Scheme 2.

On comparison of data obtained from the MALDI−TOF-MS spectra for the free radical and ATRP systems, the important observation that can be made is, since, for the ATRP systems only one pair of end groups was evident, and no chains seemed to have been initiated by the octene radicals, it can be concluded that chain transfer events, if any, in the targeted MM range were negligible.

Conclusions

The atom transfer radical copolymerization (ATRP) of methyl acrylate (MA) with 1-octene was investigated in detail. Well-controlled copolymers constituting almost 25 mol % of 1-octene were obtained using ethyl 2-bromoisobutyrate (EBriB) as initiator. Narrow molar mass distributions (MMD) were obtained for the ATRP experiments, which suggests conventional ATRP behavior, with no peculiarities caused by the incorporation of 1-octene. The feasibility of the ATRP copolymerizations was independent of the ligand employed. Copolymerizations carried out using 4,4′-dinonyl-2,2′-bipyridine (dNbpy) resulted in good control, with significant octene incorporation in the polymer. The lower overall conversion obtained for the dNbpy systems as compared to that for the PMDETA systems was attributed to the redox potential of the formed copper(I)−ligand complex. The comparable free radical (co)polymerizations (FRP) resulted in broad MMDs. Increasing the fraction of the olefin in the monomer feed led to an increase in the level of incorporation of the olefin in the copolymer, at the expense of the overall conversion.

There was a good agreement between the reactivity ratios determined for the ATRP and FRP systems.

The formation of the copolymer was established using matrix-assisted laser desorption/ionization−time-of-flight−mass spectrometry (MALDI−TOF−MS). From the obtained MALDI−TOF−MS spectra for the ATRP systems, several units of 1-octene were incorporated in the polymer chain. A gradient trend in the monomer sequence distribution was observed during the copolymerization. This was attributed to the rapidity of cross-propagation of 1-octene-terminated polymeric radicals with MA. In ATRP polymerizations, only one pair of end groups was observed. By comparison, for the FRP systems, due to the multitude of side reactions occurring, several end groups were obtained. Hence, a narrow chemical composition distribution was obtained for the ATRP systems.

Acknowledgment. The authors thank the Dutch Polymer Institute for financial support of this research. Mr. Wieb Kingma, Mr. Bastiaan Staal, and Mr. Robin Willemse are acknowledged for the SEC and MALDI−TOF−MS analysis. Mr. Jeetan Lad is acknowleged for his advice during the experimental setup for the online NMR reactions. Thanks to Dr. Michael Monteiro, Dr. Sreepadraj Karanam, and Dr. Auke Snijder for fruitful discussions during the course of this work.

Supporting Information Available: Copolymer fingerprint contour plots obtained for samples withdrawn at different time intervals during the ATR copolymerization. This material is available free of charge via the Internet at http://pubs.acs.org.

References and Notes

(1) Padwa, A. R. *Prog. Polym. Sci.* **1989**, *14*, 811.
(2) *Functional Polymers: Modern Synthetic Methods and Novel Structures*; Patil, A. O., Schulz, D. N., Novak, B. M., Eds.; ACS Symposium Series 704; American Chemical Society: Washington, DC, 1998.
(3) Johnson, L. K.; Killian, C. M.; Brookhart, M. *J. Am. Chem. Soc.* **1995**, *117*, 6414. Killian, C. M.; Temple, D. J.; Johnson, L. K.; Brookhart, M. *J. Am. Chem. Soc.* **1996**, *118*, 11664.
(4) Johnson, L. K.; Mecking, S.; Brookhart, M. *J. Am. Chem. Soc.* **1996**, *118*, 267. Mecking, S.; Johnson, L. K.; Wang, L.; Brookhart, M. *J. Am. Chem. Soc.* **1998**, *120*, 888.
(5) Wang, C.; Friedrich, S.; Younkin, T. R.; Li, R. T.; Grubbs, R. H.; Bansleben, D. A.; Day, M. W. *Organometallics* **1998**, *17*, 3149.
(6) Yasuda, H.; Furo, M.; Yamamoto, H. *Macromolecules* **1992**, *25*, 5115. Yasuda, H.; Ihara, E. *Macromol. Chem. Phys.* **1995**, *196*, 2417.
(7) Ittel, S. D.; Johnson, L. K.; Brookhart, M. *Chem. Rev.* **2000**, *100*, 1169. Boffa, L. S.; Novak, B. M. *Chem. Rev.* **2000**, *100*, 1479.
(8) Tian, G.; Boone, H. W.; Novak, B. M. *Macromolecules* **2001**, *34*, 7656.
(9) Liu, S.; Elyashiv, S.; Sen, A. *J. Am. Chem. Soc.* **2001**, *123*, 12738.
(10) Kato, M.; Kamigaito, M.; Sawamoto, M.; Higashimura, T. *Macromolecules* **1995**, *28*, 1721.
(11) Wang, J. S.; Matyjaszewski, K. *Macromolecules* **1995**, *28*, 7901.
(12) Haddleton, D. M.; Perrier, S.; Bon, S. A. F. *Macromolecules* **2000**, *35*, 8246.
(13) Keller, R. N.; Wycoff, H. D. *Inorg. Synth.* **1947**, *2*, 1.
(14) Beuermann, S.; Paquet, D. A., Jr.; McMinn, J. H.; Hutchinson, R. A. *Macromolecules* **1996**, *29*, 4206.
(15) Rudin, A. *The Elements of Polymer Science and Engineering*, 2nd ed.; Academic Press: New York, 1999; p 218.
(16) Odian, G. *Principles of Polymerization*; John Wiley: New York, 1991; p 629.
(17) Venkatesh, R.; Klumperman, B. *Macromolecules* **2004**, *37*, 1226.
(18) Xia, J.; Matyjaszewski, K. *Macromolecules* **1997**, *33*, 7697. Qui, J.; Matyjaszewski, K.; Thouin, L.; Amatore, C. *Macromol. Chem. Phys.* **2000**, *201*, 1625.
(19) Skiest, I. *J. Am. Chem. Soc.* **1946**, *68*, 1781.
(20) Chambard, G.; Klumperman, B.; Brinkhuis, R. H. G. *ACS Symp. Ser.* **2003**, *854*, 180.
(21) Mortimer, P. M.; Mortimer, G. A. *J. Macromol. Sci., Rev. Macromol. Chem* **1970**, *C4*, 281.
(22) van Herk, A. M. *J. Chem. Educ.* **1995**, *72*, 138.
(23) van den Brink, H. J. T. On-line monitoring of polymerization reactions by Raman spectroscopy. Ph.D. Thesis, ISBN 90-386-2831-5. Available from Web site Eindhoven University: http://alexandria.tue.nl/extra2/200000709.pdf.
(24) Nielen, M. W. F. *Mass Spectrom. Rev.* **1999**, *18*, 309.
(25) Matyjaszewski, K.; Nakagawa, Y.; Jasieczeck, C. B. *Macromolecules* **1998**, *31*, 1535. Coessens, V.; Matyjaszewski, K. *J. Macromol. Sci., Pure Appl. Chem.* **1999**, *A36*, 653. Coessens, V.; Matyjaszewski, K. *J. Macromol. Sci., Pure Appl. Chem.* **1999**, *A36*, 667.
(26) Axelsson, J.; Scrivener, E.; Haddleton, D. M.; Derrich, P. J. *Macromolecules* **1996**, *29*, 8875.
(27) Montaudo, G.; Montaudo, M. S.; Puglisi, C.; Samperi, F. *Rapid Commun. Mass Spectrom.* **1995**, *9*, 453; *Macromolecules* **1995**, *28*, 4562.
(28) Ahmad, N. M.; Heatley, F.; Lovell, P. A. *Macromolecules* **1998**, *31*, 2822.
(29) Moad, G.; Solomon, D. H. In *Comprehensive Polymer Science: The Synthesis, Characterization, Reactions and Applications of Polymers*; Allen, G. A., Bevington, J. C., Eds.; Pergamon Press: Oxford, England, 1989; Vol. 3, p 97.
(30) Moad, G.; Solomon, D. H. In *Comprehensive Polymer Science: The Synthesis, Characterization, Reactions and Applications of Polymers*; Allen, G. A., Bevington, J. C., Eds.; Pergamon Press: Oxford, England, 1989; Vol. 3, p 147.
(31) Chiefari, J.; Jeffery, J.; Mayadunne, R. T. A.; Moad, G.; Rizzardo, E.; Thang, S. H. *Macromolecules* **1999**, *32*, 7700.

MA035986M